Journal of Magnetism and Magnetic Materials 564 (2022) 170098

Contents lists available at ScienceDirect

Journal of Magnetism and Magnetic Materials

journal homepage: www.elsevier.com/locate/jmmm

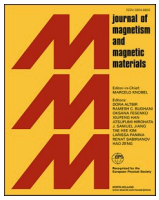

Validation of thermodynamic magneto-mechanical finite-element model on cantilever-beam type magnetostrictive energy harvester

U. Ahmed [a,*], D. Blažević [a], Y. Mizukawa [a], U. Aydin [b], P. Rasilo [a]

[a] Tampere University, Electrical Engineering Unit, P.O. Box 692, FI-33720 Tampere, Finland
[b] ABB Oy, Motion Services, P.O. Box 210, FI-00381 Helsinki, Finland

ARTICLE INFO

Keywords:
Energy harvesting
Finite element analysis
Galfenol
Magneto-elasticity
Magnetostrictive devices
Villari effect

ABSTRACT

This paper presents the validation of a thermodynamic magneto-mechanical model to analyze a galfenol based cantilever beam type energy harvesting device. As compared to some earlier modeling approaches that were tested only on specific harvester geometries, the thermodynamic model has already been validated on rod-type harvesters and is now shown to be suitable for analyzing also beam-type devices. Moreover, the paper discusses the influence of magnetostriction upon resonant frequency. The thermodynamic model is implemented in a 3D finite element solver using COMSOL Multiphysics software. This allows optimizing the device design by tuning the geometric parameters and magnetic bias under available operating conditions (amplitude and frequency of vibrations) easily and efficiently. A unimorph cantilever beam type prototype harvester device consisting of a galfenol beam bonded to an aluminum substrate is constructed for validating the model. Simulated and measured results are compared at base excitation amplitudes of 0.5 to 2 g under varying vibration frequencies. The results show that the maximum induced voltage is obtained at the resonant frequency which decreases slightly with an increase in the vibration amplitude. Furthermore, it is shown that the resonant frequency decreases from 201 Hz to 187 Hz at 1 g base acceleration when the magnetic bias is removed. The comparison of measured and simulated results show that the model can accurately predict the resonant frequency with a relative error of less than 2 %, validating the modeling approach. The model can also reasonably determine the open circuit voltage with some discrepancies at large vibration amplitudes.

1. Introduction

The concept of energy harvesting has seen significant rise in attention during the past decade as the demand for supplying maintenance and battery-free energy increased for wireless sensor nodes and small-scale power electronic devices. Rapid development of ultra-low power microelectronic sensors and integrated circuit manufacturing technology have brought the power requirement levels to tens of microwatts [1], making it possible to power electronic devices with small scale energy harvesting devices. The popular techniques of energy harvesting include piezoelectric, electromagnetic, electrostatic and magnetostrictive energy harvesting [2]. The limitations of piezoelectric harvesters are low mechanical coupling, high level of induced voltage, low output current and shorter lifespan due to mechanical breakdown at higher stress levels [3]. Frequently explored electromagnetic energy harvesters have mesoscale volumes which limits their application in small-scale power electronic devices and makes them more suitable for low frequency operation. Downscaling of this type of harvesters is also more difficult with the usual micromanufacturing techniques [4]. Electrostatic energy harvesters have mechanical limitations and need an external voltage source [4,5]. After the discovery of giant magnetostrictive materials (GMMs) such as galfenol, Terfenol-D and Metglas, the research on magnetostrictive energy harvesting has predominantly increased due to their ability to supply reliable and maintenance free energy. GMMs are rare earth alloys that show large magnetostriction and high energy density. Among GMMs, galfenol offers high tensile strength (~350 MPa), relatively large magnetostriction (200–250 ppm), low hysteresis losses and strong magneto-mechanical coupling [6]. Stefano in [7] has experimentally shown that hysteresis in galfenol-based energy harvesters is negligible. A difference of 1 % was noticed while comparing the two output power curves obtained by subsequently increasing and decreasing the applied magnetic field from 5 kA/m to 40 kA/m under constant mechanical vibrations. More importantly, galfenol is an iron gallium alloy that can be welded and machined easily, making

* Corresponding author.
E-mail address: umair.ahmed@tuni.fi (U. Ahmed).

https://doi.org/10.1016/j.jmmm.2022.170098
Received 18 August 2022; Received in revised form 6 October 2022; Accepted 19 October 2022
Available online 25 October 2022

it a more practical option in structural health condition monitoring applications. Magneto-mechanical energy harvesters utilize ambient vibrations from rotating machinery parts, rail tracks, aircraft wings, steel cable bridges etc. and converts it into electrical energy through the inverse magnetostrictive effect. Magnetostrictive harvesters can also be used as transducers for active vibration control [8] and [9].

The analysis and design of an energy harvesting device require knowledge related to the material characteristics and the operating conditions. Since such harvesters utilize vibrations from ambient sources, the information related to the nature, amplitude and frequency of the vibration is needed in the design process to determine the optimal design parameters and device geometry. The design parameters include choosing the magnetic field bias and coil parameters and constructing the device geometry based on the energy requirement for a specific application. Therefore, modeling tools are needed to analyze the harvester device under typical operating conditions in order to successfully customize the device design to the specific application [5–8].

Various models have been developed to analyze galfenol based energy harvesting devices. Models based on a linearized approach using piezomagnetic constitutive equations are presented in [9] and [10]. These models are simple to implement but incapable of analyzing the material at non-linear regions. A non-linear dynamic model based on Armstrong electro-mechanical constitutive equations is proposed in [11]. The open circuit voltage predicted by the model is higher than the measured one for large excitations (3–4 g, g = 9.81 m/s^2 being the gravitational acceleration) because the model excludes hysteresis losses. Fully coupled dynamic models implemented in finite element (FE) formulations are presented in [12] and [13]. The coupled magneto-mechanical constitutive equations describing the effect of change in magnetic flux density upon stress based on the Jiles-Atherton model are discussed in [12]. The model is validated on a cantilever beam harvester using a single base excitation value for the first four resonant frequencies to analyze the harvester output power. A two degree of freedom lumped parameter non-linear coupled magneto-mechanical model is presented in [14] where an elastic magnifier is introduced with a traditional cantilever beam harvester. This allows two resonant frequencies with magnified tip displacement to work at a lower resonant frequency. A fully coupled non-linear Gibbs free energy-based magneto-mechanical model is presented in [7]. The model is validated on a cylindrical rod type harvester device. The authors show that the model reasonably predicts the output power of 3 mW with some discrepancies.

Despite the need for a generic modeling approach that can be applied to analyze different types of magnetostrictive energy harvesters, most models presented earlier in the literature have been validated only on one specific harvester. It is thus unclear if the models are capable of accounting for the influence of the harvester geometry (e.g. rod or beam type) and different operating conditions (e.g. mechanical loading and frequency, magnetic closure circuit and magnetic field bias). In our earlier work, we have developed a thermodynamic magneto-mechanical modeling approach, implemented it in a 3D FE model using COMSOL Multiphysics, and validated it against experiments on a rod-type galfenol-based energy harvesting concept device [15,16]. This paper extends the work by validating the model with a cantilever beam type harvester. The results show that the model can also be used to reasonably predict the open circuit output voltage and resonant frequency of the cantilever beam harvester.

2. Experimental methods

2.1. Material characterization

The magneto-mechanical energy harvester utilizes galfenol produced by Extrema products as the active material which has the stoichiometry of $Fe_{81.6}Ga_{18.4}$, a polycrystalline material grown as $\langle 0\,0\,1 \rangle$ axis aligned along the length of the material. The characterization of the material is needed to identify the magneto-mechanical constitutive laws describing the magneto-elastic behavior. The detailed discussion on the experimental setup for the characterization of the material is given in [15]. In brief, a cylindrical galfenol rod of length 60 mm and diameter 12 mm is first magnetized using a 200 mHz AC voltage with the help of two sets of coils and a U-shaped iron yoke. The rod is then subjected to a static uniaxial compressive mechanical preload σ ranging from 0 to 80 MPa with a step of 5 MPa to obtain a set of magnetization (B–H) curves under stress. The magnetic field strength H is measured by a Hall probe placed in the middle of the rod whereas the magnetic flux density B is obtained by integrating the voltage induced in a pickup coil wound around the sample.

2.2. Cantilever beam energy harvester

The experimental setup of the prototype cantilever beam type energy harvesting concept device is presented in Fig. 1. A similar harvester device design is also presented in [9] and [14]. The energy harvester consists of a cantilever beam, two sets of permanent magnets and a pickup coil wound around the beam. The cantilever beam consists of a galfenol strip with a length of 60 mm, width of 6 mm and thickness of 0.78 mm. The galfenol layer acts as an active material for the energy harvester which is supported by an aluminum strip which acts as a passive substrate layer. The aluminum strip has a length of 60 mm, width of 6 mm and thickness of 1.28 mm. The galfenol and aluminum beams are glued together with a uniform thin layer of glue to avoid misalignments that can affect the bending modes of the beam.

The working principle of the experimental setup is explained with the 2D schematic diagram presented in Fig. 2. The magnetic bias is provided by two sets of 10 × 10 × 10 mm^3 neodymium magnets having remanence flux density of approximately 1.18 T. The remanence flux density is deduced by tuning the simulated magnetic field near the surface of the magnet in COMSOL to match the magnetic field measured using a Hall probe. The magnets are attached at both ends of the beam with super glue and enforced by caps made of 3D printed PETG material screwed to keep the magnets in place. The weights of the magnet and the cap are measured to be 7.57 g and 2.14 g, respectively, and together they act as the tip mass on the free end of beam. A pickup coil of 1000 turns made from 0.1 mm thick enameled copper wire is attached at the free end of the beam as shown in Fig. 1 and Fig. 2. The harvester beam is clamped to the aluminum base structure such that the active length of the cantilever beam is 38 mm from the fixed end as seen from the Fig. 2. The mechanical vibrations are provided by a Brüel & Kjær shaker device

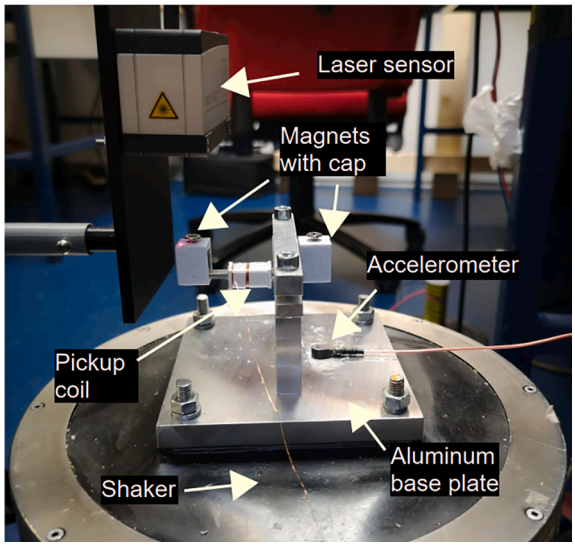

Fig. 1. The experimental setup and prototype design of the magnetostrictive energy harvester for model validation.

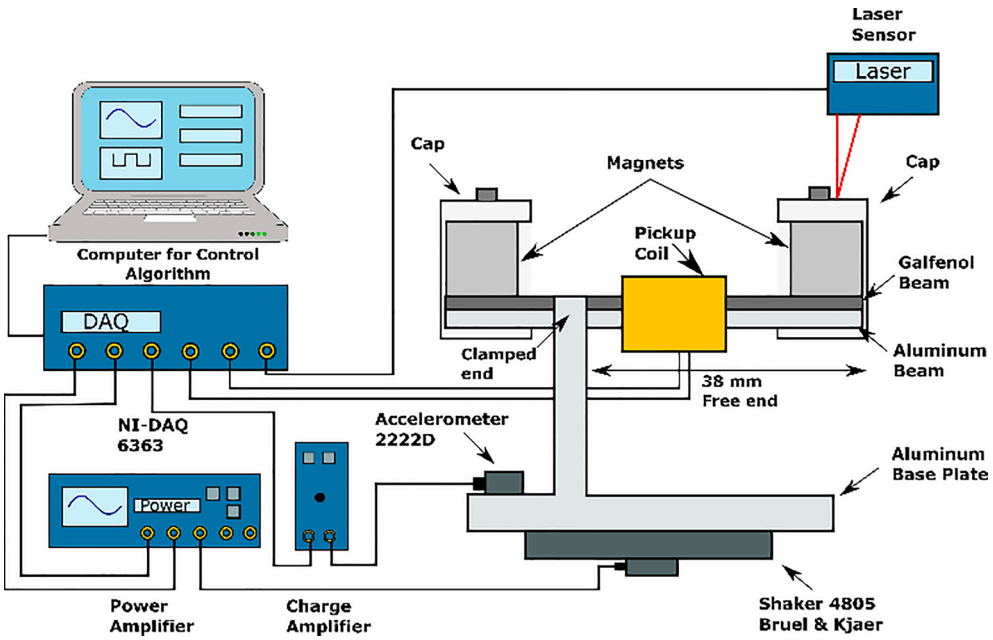

Fig. 2. Schematic diagram of the complete energy harvester setup.

that uses a permanent magnet motor (base model type 4805 with tabletop type 4813). The input signal from the shaker is supplied by a linear amplifier from Venable instruments. The shaker is able to provide peak-to-peak displacement of 13 mm at maximum 3 kHz excitation frequency. The custom-built aluminum base plate is screwed to the shaker base plate to provide a suitable rigid support for the cantilever, provide an air gap from the permanent magnet inside the shaker and securely transfer the forced sinusoidal mechanical vibrations. An optical laser displacement sensor (optoNTDC ILD1900-25) from Micro-Epsilon measures the tip displacement of the free end as shown in the Fig. 2. The laser sensor has linearity range of $< \pm 5$ μm, sampling rate of 10 kHz and its measuring range is 25 mm from the object. The vibration amplitude of the shaker plate is measured by mounting a piezoelectric accelerometer (model 2222D) which is connected to a charge amplifier from Brüel & Kjær (model type 2635) for signal conditioning.

The control algorithm is implemented in MATLAB using a National Instruments data acquisition card NI-6363. The experimental tests are performed by varying the vibration amplitudes from 0.5 g to 2 g with a step of 0.5 g. The mechanical vibration causes varying stress/strain in the beam which causes change in the magnetization of the material. A voltage is induced in the pickup coil attached to the beam as a result of the inverse magnetostrictive effect and Faraday's law. For each value of the vibration amplitude, the frequency sweep operation is performed to determine the resonant frequency of the beam by measuring the tip displacement. The amplitude of the input signal voltage supplied to the shaker is controlled by measuring the acceleration with the accelerometer attached to the aluminum base plate. The input signal is varied iteratively to obtain the desired acceleration which is then kept constant throughout the frequency sweep operation. The experiments are repeated three times to check the repeatability. The open circuit voltage, tip displacement and resonant frequency are measured to study the effect of operating frequency on the harvester performance. In this study we test the ability of the model to reproduce the effect of amplitude of mechanical vibration, magnetic bias and excitation frequency on the harvester output voltage.

3. Models

3.1. Constitutive model

The constitutive equations describing the directly-coupled multiaxial magneto-mechanical behavior in the galfenol material are derived using a thermodynamic approach, which has been presented in [17] and further discussed e.g. in [18] and [19]. The detailed discussion about implementing the approach in 3D in COMSOL Multiphysics software is presented in [15] and [16]. In brief, a Helmholtz free energy density function $\psi(\boldsymbol{B}, \boldsymbol{\varepsilon})$ is defined to describe the magneto-elastic interaction as a function of the magnetic flux density vector $\boldsymbol{B}$ and the strain tensor $\boldsymbol{\varepsilon}$. The exact form of the energy–density expression in [15–19] has varied while the model has evolved. Here it is written as

$$\psi(B,\varepsilon) = \frac{1}{2}\lambda I_1^2 + \mu I_2 + \sum_{i=1}^{\eta_\alpha} \alpha_i I_4^i + \sum_{i=1}^{\eta_\beta} \beta_i I_5^i + \sum_{i=1}^{\eta_\gamma} \gamma_i I_6^i \tag{1}$$

where α_i, β_i and γ_i are fitting parameters obtained from material characterization, and λ and μ are the Lamé parameters obtained from Young's modulus and Poisson's ratio. The total strain $\boldsymbol{\varepsilon}$ consists of the mechanical strain and the strain caused by magnetostriction. The state variables of ψ are written in terms of scalar invariants $I_1 = \mathrm{tr}(\boldsymbol{\varepsilon})$, $I_2 = \mathrm{tr}(\boldsymbol{\varepsilon}^2)$ describing linear elastic behavior, $I_4 = \boldsymbol{B}\cdot\boldsymbol{B}$ describing magnetic behavior and $I_5 = \boldsymbol{B}\cdot\boldsymbol{e}\boldsymbol{B}$ and $I_6 = \boldsymbol{B}\cdot\boldsymbol{e}^2\boldsymbol{B}$ describing magneto-mechanical behavior of the material, $\boldsymbol{e}$ being the deviatoric part of $\boldsymbol{\varepsilon}$. The constitutive equations for the magnetic field strength $\boldsymbol{H}$ and Cauchy stress tensor $\boldsymbol{\sigma}$ are then obtained by partial differentiation of the energy expression as

$$\boldsymbol{H}(\boldsymbol{B},\boldsymbol{\varepsilon}) = \left(\frac{\partial\psi}{\partial\boldsymbol{B}}\right)^{\mathrm{T}} \text{ and } \boldsymbol{\sigma}(\boldsymbol{B},\boldsymbol{\varepsilon}) = \frac{\partial\psi}{\partial\boldsymbol{\varepsilon}}. \tag{2}$$

The polynomial coefficients α_i, β_i and γ_i are determined by fitting the function $\boldsymbol{H}(\boldsymbol{B}, \boldsymbol{\varepsilon})$ obtained from (1) and (2) against the single-valued $H(B, \sigma)$ curves measured with the material characterization setup discussed in Section 2.1. During the fitting, the strain tensor $\boldsymbol{\varepsilon}$ is iterated with the Newton-Raphson method until the desired uniaxial stress is obtained. The fitting is done for the mechanical compressive preload range of 20 to 50 MPa for $\eta_\alpha = 11$, $\eta_\beta = 1$ and $\eta_\gamma = 2$ and the coefficient of the fitting parameters are given in [16].

3.2. Finite element model

The analytical expressions of the constitutive equations (1)-(2) are implemented in a 3D FE solver in COMSOL by overriding the electromagnetic and mechanical constitutive equations. The detailed discussion for the model implementation is presented in [16]. The 3D magneto-mechanical FE simulation for a cantilever beam type harvester is carried out for one half of the geometry, which is presented in Fig. 3. The model is constructed based on the actual prototype harvester device which consists of the galfenol beam attached to the aluminum beam, two permanent magnets at both ends and a pickup coil wound around the beam. In the COMSOL model, the solid mechanics interface solves for the equation of motion which includes the material damping written as

$$\rho\left(\frac{d^2\boldsymbol{u}}{dt^2}+\alpha_{\mathrm{dM}}\frac{d\boldsymbol{u}}{dt}\right)-\nabla\cdot\left(\boldsymbol{\sigma}(\boldsymbol{B},\boldsymbol{\varepsilon})+\beta_{\mathrm{dK}}\frac{\partial\boldsymbol{\sigma}(\boldsymbol{B},\boldsymbol{\varepsilon})}{\partial t}\right)=0 \tag{3}$$

where $\boldsymbol{u}$ is the displacement vector, ρ is the mass density, and α_{dM} and β_{dk} are the mass and stiffness damping parameters, respectively. The mechanical damping is simulated as Rayleigh damping expressed as

$$\zeta=\frac{1}{2}\left(\frac{\alpha_{\mathrm{dM}}}{2\pi f_0}+\beta_{\mathrm{dK}}2\pi f_0\right). \tag{4}$$

The damping ratio ζ and the resonant frequency f_0 are experimentally obtained from a free vibration test. The damping is assumed to consist mainly of the material-related damping β_{dk}, which is obtained from (4) by setting $\alpha_{\mathrm{dM}}=0$.

The normal component of displacement u_{y} is set to zero at the sliced boundary. The sinusoidal mechanical vibration amplitude ranging from 0.5 g to 2 g is imposed by prescribing the normal component of the displacement u_{z} on the aluminum clamp domain. The tip mass of 9.71 g is realized utilizing an added mass node to the magnet domain at the free end of the beam. The electromagnetic fields are computed by adding the magnetic field interface which solves the Maxwell's equations. The remanence flux density of the permanent magnets is the set as 1.18 T.

In the galfenol material, the combination of Ampere's and Faraday's laws is solved in terms of the magnetic vector potential $\boldsymbol{A}$ as

$$\nabla\times\boldsymbol{H}(\boldsymbol{B},\boldsymbol{\varepsilon})+\kappa\frac{\partial\boldsymbol{A}}{\partial t}=0 \tag{5}$$

where κ denotes the electrical conductivity. In the other regions, a purely electromagnetic problem is solved as

$$\nu\nabla\times\nabla\times\boldsymbol{A}+\kappa\frac{\partial\boldsymbol{A}}{\partial t}=\nabla\times\boldsymbol{H}_{\mathrm{c}} \tag{6}$$

where ν is the constant reluctivity and $\boldsymbol{H}_{\mathrm{c}}$ is the coercive field of the magnets. The voltage V_{ind} induced into the pickup coil is computed by averaging the time derivative of the circumferential component of the magnetic vector potential $\boldsymbol{A}$ over all possible paths in the cylindrical coil volume Ω_{coil} as

$$V_{\mathrm{ind}}=\frac{N}{S_{\mathrm{coil}}}\int_{\Omega_{\mathrm{coil}}}\frac{\partial\boldsymbol{A}_\theta}{\partial t}d\Omega \tag{7}$$

where N is the number of coil turns and S_{coil} is the cross-section area of the coil domain. The time integration is done using the Generalized Alpha method (a second order backward differential formulation with a parameter to control the damping of higher frequencies) instead of Backward Euler method since the latter causes numerical damping at higher frequencies [20]. The resulting non-linear system is solved using the Newton Raphson method.

4. Results and discussion

4.1. Material characterization

The energy density function ψ is fitted to the single-valued measured $H(B,\sigma)$ curves obtained from the material characterization setup discussed in Section 2.1. The comparison of the measured and fitted curves is presented in Fig. 4. The fitting is performed for the preload range of 20 to 50 MPa shown in Fig. 4. The preload range of 20 to 50 MPa is chosen as it provides a relatively good fitting against the measured B–H curves from 0 to 80 MPa explained in [16] which also contains the coefficients of the fitting parameters.

4.2. Beam resonant frequency

As discussed in Section 1, optimizing the energy harvester design requires knowledge related to operating conditions including the resonant frequency, magnetic bias etc. From literature [9] it is known that maximum power is generated when the cantilever beam operates at the resonant frequency. For the energy harvesting setup discussed in Section 2.2, the resonant frequency of the beam is first calculated analytically as

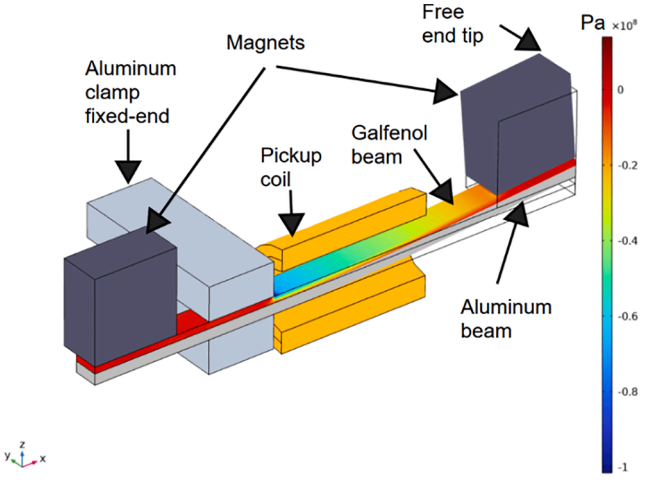

Fig. 3. The geometry of the model implemented in COMSOL for 3D FE simulation. Color bar denotes xx-component of stress in the galfenol beam (Pa).

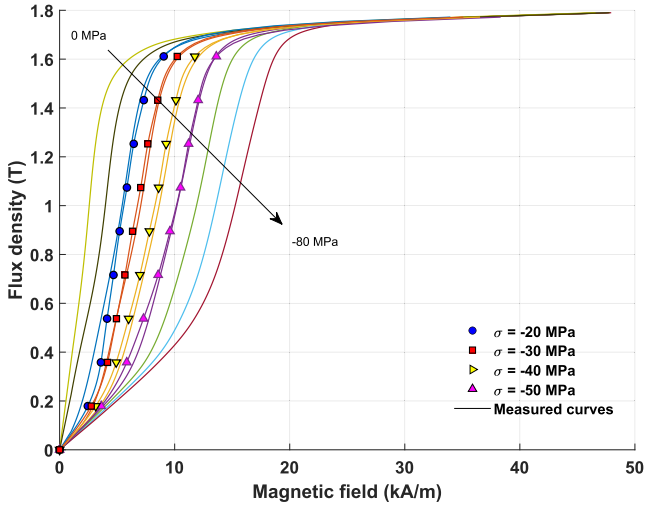

Fig. 4. Comparison among measured (solid lines) and fitted (lines with markers) magnetization curves B–H under different values of static compressive preload (σ).

$$f_0 = \frac{1}{2\pi}\sqrt{\frac{3EI}{(M + m_{\text{eff}})l^3}} \tag{8}$$

where E is the effective Young's modulus taken as 70 GPa for the combined galfenol-aluminum beam, M is the tip mass of 9.71 g including the PEGT caps whereas m_{eff} is the effecting beam mass of 2.2 g. The term l denotes the effective beam length of 38 mm and I is the second moment of inertia. The resonant frequency calculated from (8) is 189 Hz.

Experimentally, the resonant frequency with magnets attached at both ends is then obtained from free vibrations by measuring the decaying amplitude of the tip displacement presented in Fig. 5. The free vibrations are measured using a precision laser displacement sensor. The damping ratio ζ is computed from the free vibrations using a logarithmic decrement method as

$$\zeta = \frac{\ln\left(\frac{X_k}{X_{k+n}}\right)}{2\pi n} \tag{9}$$

where X_k and X_{k+n} are the k^{th} and $(k + n)^{\text{th}}$ values of the peak displacement amplitude. A resonant frequency of 200 Hz is obtained by measuring a time of 200 ms over $n = 8$ consecutive periods as indicated in the Fig. 5. A damping ratio of $\zeta = 0.0145$ is deduced for the corresponding peaks of the free vibrations.

Next, two sets of experiments are performed to determine the effect of magnetostriction on the resonant frequency. In case of forced vibrations, the resonant frequency is measured using a frequency sweep method by applying sinusoidal vibrations of 1 g acceleration. The first test is performed when the beam is magnetized by the permanent magnets, sweeping the frequency around the resonant frequency of 200 Hz obtained from the free vibration test. The second test is performed when the magnets are replaced by iron cubes with exactly the same weight as the magnets, sweeping the frequency around the analytically calculated resonant frequency of 189 Hz. A resonant frequency of 201 Hz is obtained with the magnets, and a resonant frequency of 187 Hz is obtained with the iron cubes at 1 g acceleration shown in Fig. 6 (a) and (b), which indicates that the magnetostriction increases the resonant frequency. The increase in resonant frequency can be explained by the so-called ΔE effect which states that the Young's modulus of the magnetostrictive material increases due to magnetization as discussed in [21] and [22]. According to (8), the increasing Young's modulus increases the resonant frequency.

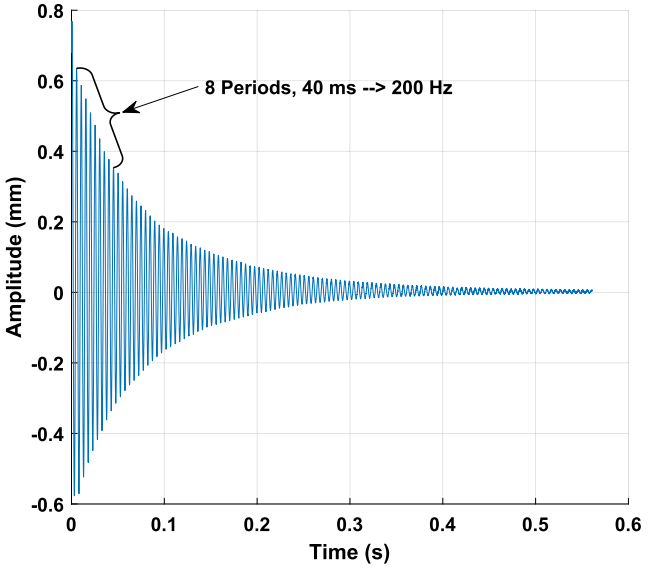

Fig. 5. Measured tip displacement at free vibration. The measured resonant frequency deduced from free vibration is 200 Hz.

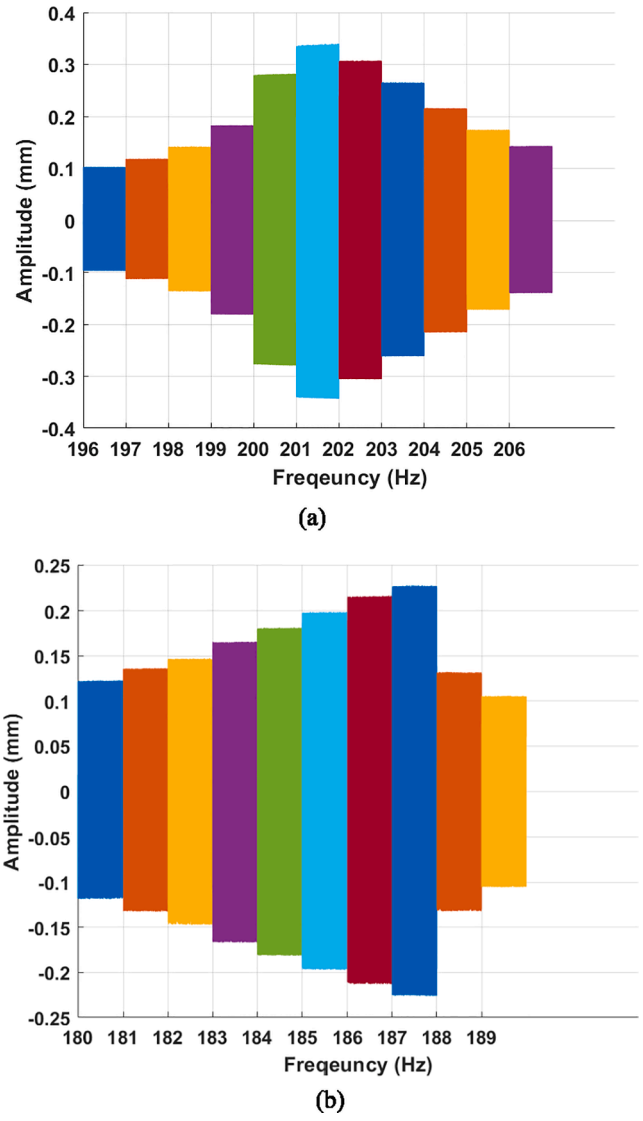

Fig. 6. Measured tip displacement under 1 g acceleration using the frequency sweep method. A resonant frequency of 201 Hz is obtained with magnets (a) and 187 Hz with iron cubes (b).

For the FE simulations in COMSOL, the mechanical damping is realized using Rayleigh damping presented in (4) where f_0 is kept constant at 201 Hz (obtained from the frequency sweep) throughout the simulations. The FE simulation is performed with and without magnetostriction to validate the thermodynamic model and to compare the results. A resonant frequency of 200 is computed with magnetostriction whereas a resonant frequency of 184 Hz is computed without magnetostriction using the magneto-mechanical model. This illustrates that the model can successfully predict the change in the resonant frequency due to magnetostriction. The comparison among measured, simulated and analytically calculated resonant frequencies showing the effect of magnetostriction is given in Table 1.

Table 1
Comparison of measured, simulated and analytically calculated resonant frequencies at 1 g.

	Measured	Simulated	Analytical
With magnetostriction	201 Hz	200 Hz	–
Without magnetostriction	187 Hz	184 Hz	189 Hz

4.3. Energy harvesting setup

The comparison of the measured and simulated open circuit voltage (rms) and tip displacement showing the influence of mechanical vibration amplitude and frequency is presented in Figs. 7 and 8. The results are obtained by applying forced mechanical vibrations from 0.5 g to 2 g for the frequency range of 196 Hz to 206 Hz. The results show that the output voltage is maximum at the resonant frequency which decreases slightly with the increase in the amplitude of the mechanical vibrations. The experiments are repeated three times keeping the same input conditions to check the repeatability. The deviations can be seen among the measured experimental results from Fig. 7 (a) and Fig. 8 (a) shown as markers, whereas the solid lines indicate the mean value. The deviation is large near the resonant frequency for the 1.5 g and 2 g excitations. This is caused by a large tip displacement due to high acceleration considering the size of the beam, which makes it difficult to stabilize near the resonant frequency.

As discussed earlier, the harvester utilizes ambient vibrations whose frequency and amplitude cannot be controlled. Therefore, the proposed model can be used to optimize the geometry and tip mass such that the harvester operates at the resonant frequency for peak performance. The comparison among measured and simulated results depicts that the thermodynamic model can accurately predict the resonant frequency with a percentage error of less than 2 %. Moreover, the results show that the resonant frequency decreases slightly with the increase in the vibration amplitude from 202 Hz to 198 Hz also predicted by the simulated results in Fig. 7 and Fig. 8.

The difference in the amplitudes of the measured and simulated displacement is caused by the damping ratio which is chosen to be frequency independent in FE simulations throughout the frequency sweep. Changing the damping ratio directly affects the tip displacement and hence the output voltage. The simulated output voltage is also affected by the magnetic bias which is estimated by measuring the magnetic field using a Hall sensor. Furthermore, the simulations do not account for the thickness of glue or the small airgaps between the caps holding the magnets at both ends. In addition, the output voltage is found sensitive to the placement of the pickup coil over beam, slight displacement of the permanent magnets and the cantilever's support clamping strength of the aluminum base also affects the resonant frequency and tip displacement. Therefore, the comparison of measurement and simulated results should be done keeping in mind the sensitivity in the

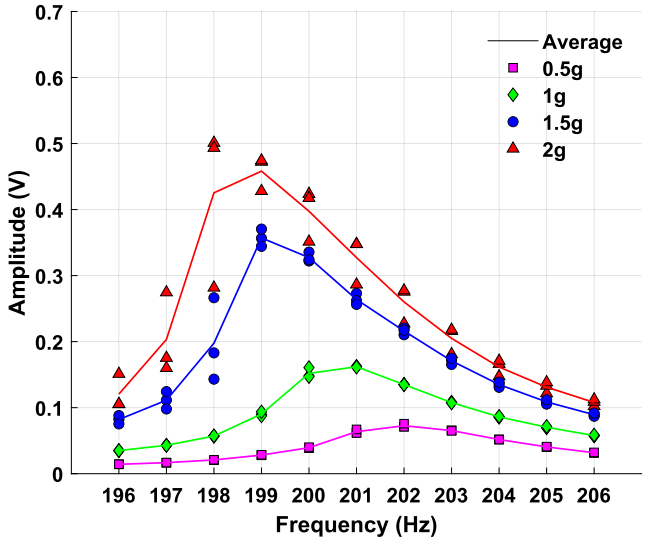

(a)

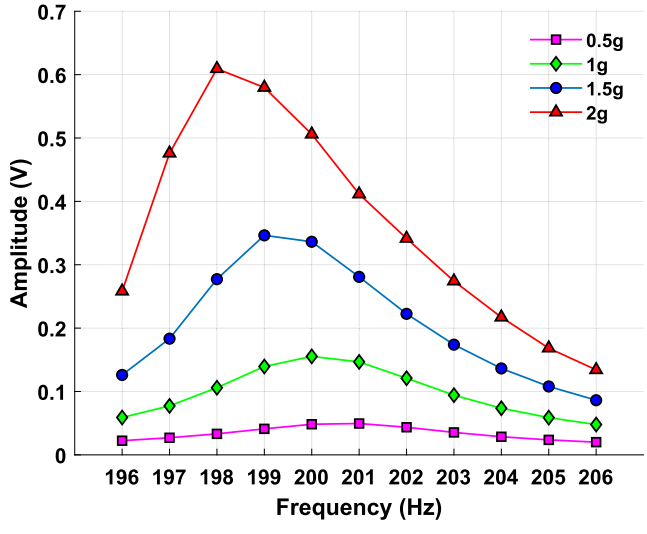

(b)

Fig. 7. Measured (a) and simulated (b) open circuit voltage (rms) curves under varying amplitude of mechanical vibrations.

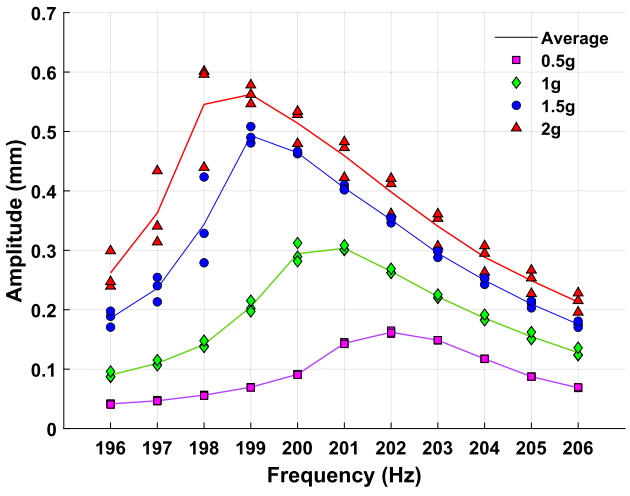

(a)

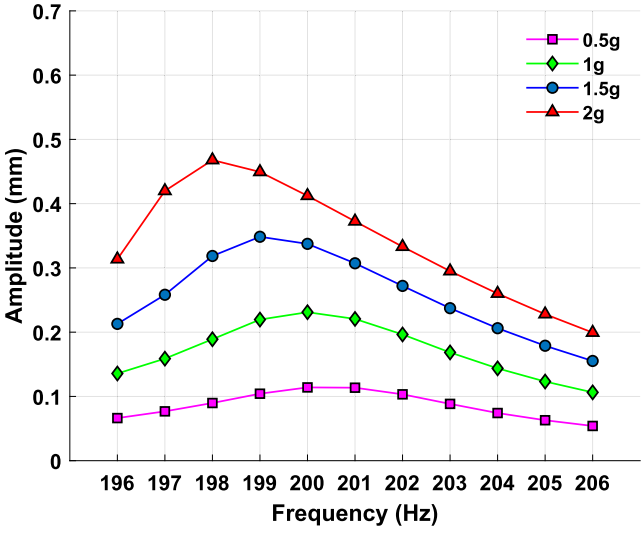

(b)

Fig. 8. Measured (a) and simulated (b) tip displacement measured from laser sensor.

measurements and limitations of the model.

5. Conclusion

In this paper, a thermodynamic magneto-mechanical modeling approach has been successfully validated against measurements from a cantilever beam type prototype energy harvester device. The model has previously been validated to analyze a cylindrical rod type harvester [15] which was modified later to include a magnetic closure circuit with varying magnetic field bias discussed in [16]. The thermodynamic model has been implemented in COMSOL Multiphysics software for 3D FE simulations. The advantage of implementing the model in COMSOL is the ability to conveniently modify the harvester geometry and perform parametric sweep operations to analyze the performance of the harvester for device optimization. Comparison of the simulated and measured results indicates that the model can accurately predict the resonant frequency of the harvester yielding maximum performance and determine the output voltage under varying vibration amplitudes and frequencies.

The FE simulations are performed considering no airgap between the magnets and the beam and a strong mechanical contact between the galfenol and aluminum beams which is an ideal condition that differs from the actual setup which uses adhesive and mechanical means of attachment. For comparison, the model needs to be tuned in order to consider the exact mechanical stresses in the beam and magnetic field bias which is not practical for each mechanical loading case. Furthermore, it is concluded that comparison of the measured and simulated results requires repeatable measurements which should be ensured by maintaining a constant clamping position of the cantilever beam, coil placement and magnet displacement. However, the measurement repeatability suffers near resonant frequency at high vibration amplitude caused by slight displacement of the tip magnet which changes the mechanical damping.

Modeling tools are required to determine the optimal design characteristic (harvester geometry, coil parameters, magnetic bias etc.) under available operating conditions (vibration amplitude, nature and frequency of mechanical vibrations) to analyze the energy harvester device and then optimize it to obtain peak performance. Combining the results of this paper to those of [15] and [16], the thermodynamic modeling approach has been validated to be suitable as a generic tool for analyzing different types of magnetostrictive energy harvesting devices. For a cantilever beam type harvester geometry, the model is able determine the resonant frequency and open circuit voltage yielding maximum harvester potential. For cylindrical rod type harvester, the model is able to successfully determine the optimal static mechanical preload σ, magnetic bias and optimal value of load resistance to obtain the maximum output power under forced sinusoidal mechanical excitations. The presented modeling approach can thus be used to support the design of energy harvesters for different applications.

CRediT authorship contribution statement

U. Ahmed: Conceptualization, Software, Methodology, Investigation, Writing – original draft. **D. Blažević:** Investigation, Writing – review & editing, Supervision. **Y. Mizukawa:** Investigation. **U. Aydin:** Formal analysis, Software. **P. Rasilo:** Formal analysis, Supervision, Writing – review & editing.

Declaration of Competing Interest

The authors declare that they have no known competing financial interests or personal relationships that could have appeared to influence the work reported in this paper.

Data availability

No data was used for the research described in the article.

Acknowledgements

The authors would like to thank the materials science and environmental engineering group of Tampere University for their assistance with this work. Also, we would like to thank the funding organizations including the European Union's Horizon 2020 research and innovation programme (Marie Skłodowska-Curie grant No 838375), Aimo Puromäki special funds (No. 20200522) awarded by the KAUTE foundation and the Finnish Government Scholarship Pool (No. KM-20-11380) awarded by the Finnish National Agency for Education for supporting this reseach work.

References

[1] X. Tang, X. Wang, R. Cattley, F. Gu, A.D. Ball, Energy harvesting technologies for achieving self-powered wireless sensor networks in machine condition monitoring: a review, Sensors 18 (12) (2018) 4113.
[2] H. Liu, C. Cong, Q. Zhao, K. Ma, Comprehensive analysis of the energy harvesting performance of a fe-ga based cantilever harvester in free excitation and base excitation mode, Sensors 19 (15) (2019) 3412.
[3] P.V. Avvari, Y. Yang, C.K. Soh, Long-term fatigue behavior of a cantilever piezoelectric energy harvester, J. Intell. Mater. Syst. Struct. 28 (9) (2017) 1188–1210.
[4] J. Siang, M.H. Lim, M. Salman Leong, Review of vibration-based energy harvesting technology: mechanism and architectural approach, Int. J. Energy Res. 42 (5) (2018) 1866–1893.
[5] M. Iqbal, M.M. Nauman, F.U. Khan, P.E. Abas, Q. Cheok, A. Iqbal, B. Aissa, Vibration-based piezoelectric, electromagnetic, and hybrid energy harvesters for microsystems applications: a contributed review, Int. J. Energy Res. 45 (1) (2021) 65–102.
[6] V. Berbyuk, Vibration energy harvesting using Galfenol-based transducer, in: Active and Passive Smart Structures and Integrated Systems vol. 8688, SPIE, 2013, pp. 429–440.
[7] S. Palumbo, P. Rasilo, M. Zucca, Experimental investigation on a Fe-Ga close yoke vibrational harvester by matching magnetic and mechanical biases, J. Magn. Magn. Mater. 469 (2019) 354–363.
[8] C.S. Clemente, A. Mahgoub, D. Davino, C. Visone, Multiphysics circuit of a magnetostrictive energy harvesting device, J. Intell. Mater. Syst. Struct. 28 (17) (2017) 2317–2330.
[9] J.H. Yoo, A.B. Flatau, A bending-mode galfenol electric power harvester, J. Intell. Mater. Syst. Struct. 23 (6) (2012) 647–654.
[10] X. Zhao, D.G. Lord, Application of the Villari effect to electric power harvesting, J. Appl. Phys. 99 (8) (2006) 08M703.
[11] S. Cao, J. Zheng, Y. Guo, Q. Li, J. Sang, B. Wang, R. Yan, Dynamic characteristics of Galfenol cantilever energy harvester, IEEE Trans. Magn. 51 (3) (2015) 1–4.
[12] P.G. Evans, M.J. Dapino, Dynamic model for 3-D magnetostrictive transducers, IEEE Trans. Magn. 47 (1) (2010) 221–230.
[13] S. Chakrabarti, M.J. Dapino, Coupled axisymmetric finite element model of a hydraulically amplified magnetostrictive actuator for active powertrain mounts, Finite Elem. Anal. Des. 60 (2012) 25–34.
[14] S. Cao, L. Liu, J. Zheng, R. Pan, G. Song, Modeling and analysis of Galfenol nonlinear cantilever energy harvester with elastic magnifier, IEEE Trans. Magn. 55 (6) (2019) 1–5.
[15] U. Ahmed, J. Jeronen, M. Zucca, S. Palumbo, P. Rasilo, Finite element analysis of magnetostrictive energy harvesting concept device utilizing thermodynamic magneto-mechanical model, J. Magn. Magn. Mater. 486 (2019) 165275.
[16] U. Ahmed, U. Aydin, M. Zucca, S. Palumbo, R. Kouhia, P. Rasilo, Modeling a Fe-Ga energy harvester fitted with magnetic closure using 3D magneto-mechanical finite element model, J. Magn. Magn. Mater. 500 (2020) 166390.
[17] K. Fonteyn, A. Belahcen, R. Kouhia, P. Rasilo, A. Arkkio, FEM for directly coupled magneto-mechanical phenomena in electrical machines, IEEE Trans. Magn. 46 (8) (2010) 2923–2926.
[18] P. Rasilo, D. Singh, U. Aydin, F. Martin, R. Kouhia, A. Belahcen, A. Arkkio, Modeling of hysteresis losses in ferromagnetic laminations under mechanical stress, IEEE Trans. Magn. 52 (3) (2015) 1–4.
[19] P. Rasilo, D. Singh, J. Jeronen, U. Aydin, F. Martin, A. Belahcen, L. Daniel, R. Kouhia, Flexible identification procedure for thermodynamic constitutive models for magnetostrictive materials, Proc. R. Soc. A 475 (2223) (2019) 20180280.
[20] Z. Deng, M.J. Dapino, Multiphysics modeling and design of Galfenol-based unimorph harvesters, in: Industrial and Commercial Applications of Smart Structures Technologies, vol. 9433, SPIE, 2015, pp. 74–83.
[21] M. Löffler, R. Kremer, A. Sutor, R. Lerch, Hysteresis of the resonance frequency of magnetostrictive bending cantilevers, J. Appl. Phys. 117 (17) (2015) 17A907.
[22] L. Daniel, O. Hubert, An analytical model for the ΔE effect in magnetic materials, Eur. Phys. J.-Appl. Phys. 45 (3) (2009) 31101.